

Surface Phase Transitions Induced by Electron Mediated Adatom-Adatom Interaction

Junren Shi¹, Biao Wu^{1,2}, X.C. Xie^{3,4}, E.W. Plummer^{1,5}, Zhenyu Zhang^{1,5}

¹Condensed Matter Sciences Division, Oak Ridge National Laboratory, Oak Ridge, Tennessee 37831

²Department of Physics, University of Texas, Austin, Texas 78712

³Department of Physics, Oklahoma State University, Stillwater, Oklahoma 74078

⁴International Center for Quantum Structures, Chinese Academy of Sciences, Beijing 100080, China

⁵Department of Physics, University of Tennessee, Knoxville, Tennessee 37996

We propose that the indirect adatom-adatom interaction mediated by the conduction electrons of a metallic surface is responsible for the $\sqrt{3} \times \sqrt{3} \leftrightarrow 3 \times 3$ structural phase transitions observed in Sn/Ge (111) and Pb/Ge (111). When the indirect interaction overwhelms the local stress field imposed by the substrate registry, the system suffers a phonon instability, resulting in a structural phase transition in the adlayer. Our theory is capable of explaining all the salient features of the $\sqrt{3} \times \sqrt{3} \leftrightarrow 3 \times 3$ transitions observed in Sn/Ge (111) and Pb/Ge (111), and is in principle applicable to a wide class of systems whose surfaces are metallic before the transition.

PACS numbers: 68.35.Bs, 68.35.Rh, 73.20.At, 71.45.Lr

Over the years, a great deal of efforts have been devoted to experimental studies of structural phase transitions at surfaces. One compelling example is the $\sqrt{3} \times \sqrt{3} \leftrightarrow 3 \times 3$ transitions in the 1/3 monolayer of Pb or Sn on Ge(111) directly observed by the Scanning Tunneling Microscopy (STM) [1, 2, 3] (see Fig. 1). These studies have stimulated an active line of theoretical research, yet to date, the precise nature and the underlying mechanism of such transitions are still highly controversial. The original paper attributed this transition to a Charge Density Wave (CDW) driven by two-dimensional Fermi surface nesting [1, 2]. Subsequent papers have attributed the transition to a Kohn Anomaly [4], bond density waves [5], a pseudo Jahn-Teller transition [6, 7], a surface Mott insulator [8], dynamical fluctuations [9], a soft phonon [10] and most recently to disproportionation [11]. Although all these theories are successful to certain extent, a unified microscopic picture is yet to emerge. The issue becomes even more intriguing after the observation of the delicate role of defects in the transition [12, 13].

In this Letter, we present a new mechanism for surface phase transitions, which places central emphasis on the indirect adatom-adatom interaction mediated by the two-dimensional conduction electrons of a metallic surface. In

this theory, when the conduction-electron mediated adatom-adatom interaction overwhelms the local stress field imposed by the substrate registry, the system suffers a phonon instability, leading to a structural phase transition. The theory is capable of explaining all the salient features of the transition observed in Sn/Ge (111), including the appearance of surface charge density waves and the delicate role of surface defects. It also predicts the existence of a glassy phase in such systems.

The electron-mediated adatom-adatom interaction originates from the tendency of the conduction electrons to screen external disturbances. In the case of adlayer systems such as Sn/Ge (111), the dangling bond electrons of the adatoms form a quasi two-dimensional (2D) electron gas at the surface. The movement of an adatom disturbs the electron gas, which responds in the form of Friedel oscillations in its density. Such charge corrugations propagate at the surface to reach other adatoms, thereby establishing an indirect interaction between adatoms. We note that the basic physical concept emphasized here has found important applications in several other fields, such as the RKKY interaction between spins [14] and chemisorption of adatoms at metal surfaces [15, 16, 17].

We stress that, the central ingredients of the picture developed here are the existence of surface conduction electrons and their capability of coupling with the displacement of the adatoms (electron-phonon coupling). Both are evidently present in Sn/Ge (111) and Pb/Ge (111). As shown in Fig. 1, each Sn adatom bonds to three Ge substrate atoms directly under it, leaving one bond dangling. The electrons in the dangling bonds are localized in the surface and form a 2D electron system with a narrow (~ 0.5 eV) half-filled band. When an adatom is displaced, the angles between the dangling bond and its three saturated Sn-Ge bonds have to adjust accordingly, inducing a variation in the s-p hybridization of the electron states of the Sn adatom, and a corresponding change in the energy of the dangling state [18]. This process can be described by the Holstein electron-phonon coupling [19], where the dangling state energy of an adatom depends on its displacement as $\epsilon_d = \epsilon_0 - \beta z$, with z being the displacement of the

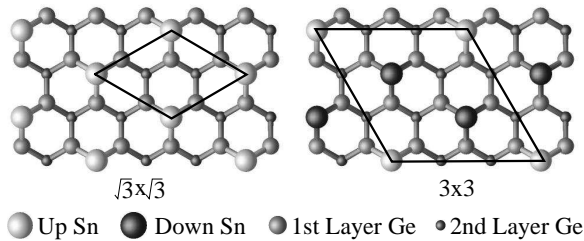


Figure 1: Structures of $\sqrt{3} \times \sqrt{3}$ (left) and 3×3 (right) phases of Sn/Ge(111). In the experiment, one third monoatomic layer of tin was deposited onto a Ge(111) surface, and a gradual transition from the room-temperature flat $\sqrt{3} \times \sqrt{3}$ phase to the low-temperature 3×3 phase was observed [1, 2]. In the new phase, one Sn adatom moves up and two move down in each 3×3 unit cell.

adatom along the direction perpendicular to the surface, and β a positive constant, reflecting that a downward displacement induces a higher dangling state energy.

The total Hamiltonian of the system is written as,

$$H = \sum_{i,s} (\epsilon_0 - \beta z_i) c_{is}^\dagger c_{is} - t \sum_{\langle ij \rangle, s} c_{is}^\dagger c_{js} + \frac{\alpha}{2} \sum_i z_i^2 + \dots, \quad (1)$$

where z_i is the displacement of the adatom located at site i , and c_{is}^\dagger (c_{is}) is the creation (annihilation) operator of a dangling bond electron at site i and with spin s . The hopping constant t is between nearest neighbors and can be regarded as independent of the adatom displacement because the leading correction term is second order in z_i . The term involving α is the elastic energy of the lattice distortion caused by the displacements of the adatoms, which represents the local stress field imposed by the substrate. In Eq. 1, the higher order terms in z_i are ignored for the moment. As it will become clear in later discussions, Eq. 1 is sufficient for determining the structural stability of the system, while the higher order terms are important only in stabilizing the system after the system becomes unstable.

The stability of the $\sqrt{3} \times \sqrt{3}$ phase can be examined within the perturbation theory by expanding the total energy change up to the second order in the adatom displacements,

$$\Delta E = \frac{\alpha}{2} \sum_i z_i^2 - \beta \langle n \rangle \sum_i z_i - \frac{1}{4} \sum_{ij} J_{ij} (z_i - z_j)^2 + \mathcal{O}(z^3), \quad (2)$$

where $\langle n \rangle$ is the average number of the dangling electrons for each adatom, and J_{ij} are the coupling coefficients for the indirect adatom-adatom interaction. In the continuum limit, we have,

$$\begin{aligned} J_{ij} &= 8\beta^2 \sum_{\epsilon_{\mathbf{q}} < \epsilon_F} \sum_{\epsilon_{\mathbf{k}} > \epsilon_F} \frac{\exp[-i(\mathbf{q} - \mathbf{k}) \cdot (\mathbf{R}_i - \mathbf{R}_j)]}{\epsilon_{\mathbf{q}} - \epsilon_{\mathbf{k}}} \\ &\approx \frac{8n^2\beta^2}{\epsilon_F} F(k_F |\mathbf{R}_i - \mathbf{R}_j|) \end{aligned} \quad (3)$$

where $\epsilon_{\mathbf{q}}$ ($\epsilon_{\mathbf{k}}$) is the energy dispersion of the electron band, ϵ_F is the Fermi energy relative to the band bottom and contains implicitly the hopping constant t . The coefficients J_{ij} are the same as for the 2D RKKY coupling [20], and are oscillatory spatially with an asymptotic dependence of $-\sin(2k_F r)/r^2$, as shown in Fig. 2(a). When applied to the case of $\sqrt{3} \times \sqrt{3}$ structure of Sn/Ge(111), the coupling between the nearest neighbors is positive; therefore, the interaction is anti-ferromagnetic-like, namely, two nearest neighboring adatoms tend to displace in opposite directions.

Keeping only the interacting terms between nearest neighbors, we can reduce Eq. 2 to

$$\Delta E = \frac{1}{2}(\alpha - 6J_1) \sum_i \tilde{z}_i^2 + \frac{J_1}{2} \sum_{\langle ij \rangle} \tilde{z}_i \tilde{z}_j + \mathcal{O}(\tilde{z}^3), \quad (4)$$

where $\tilde{z}_i = z_i - \beta/(\alpha \langle n \rangle)$. This equation shares the same form as the phenomenological charge compensate model (CCM)

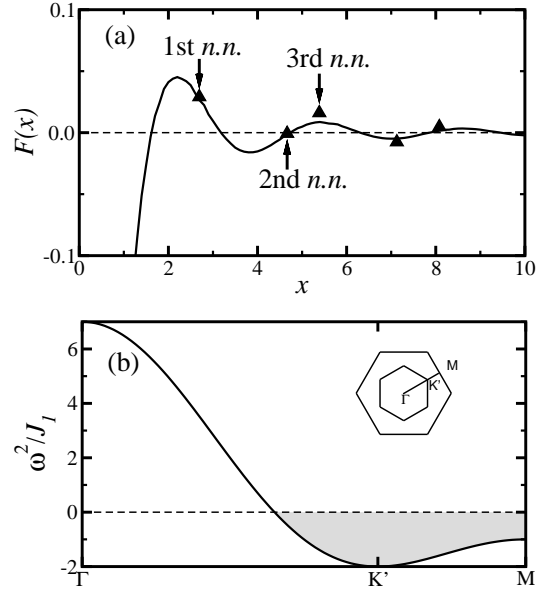


Figure 2: (a) $F(x)$ in Eq. 3 (as a comparison, the triangles are the results of tight-binding calculations up to the fifth nearest neighbors for the $\sqrt{3} \times \sqrt{3}$ structure). In this system, the Fermi momentum $k_F \approx \sqrt{2\pi\rho} = \sqrt{4\pi}/(3^{1/4}a)$, where ρ is the density of the surface electrons, a is the lattice constant. (b) Phonon dispersion [Eq. 4] along the direction ΓM shown in the inset, with $\alpha/J_1 = 7$. The shaded area indicates the unstable phonon modes, of which the most unstable K' mode defines the 3×3 periodicity.

proposed by Melechko et al. [21], which has been shown to be capable of interpreting most of the experimental STM images. Our theory thus provides the microscopic mechanism behind the success of the CCM model. We note that the long-range terms in Eq. 2 should be included in future investigation of large-scale phenomena such as domain wall formation, but they do not alter the nature of the phase transitions, which is the focus of the present study.

From Eq. 4, it is evident that the system becomes unstable against adatom displacements when the elastic restoring force is weak. This can be illustrated with the phonon dispersion of Eq. 4 [10]:

$$\omega^2 = \alpha - 6J_1 + J_1 \sum_l \cos(\mathbf{k} \cdot \mathbf{R}_l), \quad (5)$$

where the sum is over six nearest neighbors. When $\alpha/J_1 < 9$, ω becomes imaginary for certain \mathbf{k} vectors (Fig. 2b), indicating that the corresponding phonon modes become unstable (phonon catastrophe) and the system is driven into new phases. Note that the soft phonon picture suggested in Ref. 10 is a very special case of our model, occurring only when α/J_1 is exactly equal to 9. Furthermore, the phonon instability established here does not require any special properties of the Fermi surface such as the Fermi surface nesting, nor does it rely on the inclusion of electron-electron correlations, which is the focus of most of the earlier efforts with little success [8, 22].

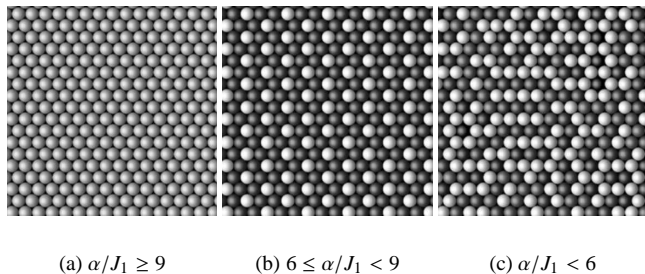


Figure 3: Schematic images of the stable configurations for different parameter regimes. (a) $\sqrt{3} \times \sqrt{3}$ phase; (b) 3×3 phase; (c) kinked-line phase.

Higher order terms become important when the system enters the unstable regime. On a microscopic level, those terms may arise from a variety of sources, such as anharmonicity in the elastic energy, finite width of the electron band, higher order terms in expansions of the site energy and the hopping constant t . The precise form of these higher order terms may affect the quantitative details of the phase transition, such as the amplitudes of the adatom displacements and preference among the nearly degenerate ground states, but the occurrence and nature of the transition is totally determined by the intrinsic instability represented in Eq. 4. For this reason and also for simplicity, we assume that the higher order terms mainly come from the anharmonic terms of the on-site elastic energy,

$$-\frac{\delta}{3} \sum_i \tilde{z}_i^3 + \frac{\gamma}{4} \sum_i \tilde{z}_i^4 \quad (6)$$

where $\delta > 0$ and $\gamma > 0$. δ is positive, because displacing an adatom out of the surface weakens the bond strengths between the adatom and the substrate atoms.

By adding those higher order terms into Eq. 4, we can determine the stable configurations. The numerical results are shown in Fig. 3. The ratio α/J_1 is a crucial deterministic parameter for the phase transition. When $\alpha/J_1 \geq 9$, the ground state is the flat $\sqrt{3} \times \sqrt{3}$ phase. When $6 \leq \alpha/J_1 < 9$, the ground state is the 3×3 phase in the one up-two down configuration: in each unit cell of the 3×3 lattice, one Sn adatom moves up (z_\uparrow), while the other two move down (z_\downarrow), and the displacements satisfy $z_\uparrow \approx 2|z_\downarrow|$. The nearly degenerate one down-two up configuration has a higher energy due to the cubic term in Eq. 6. Such 3×3 patterns were also observed experimentally [7, 23]. Note that the 3×3 structure corresponds to the most unstable phonon mode in Eq. 5, as demonstrated in Fig. 2(b).

When $\alpha/J_1 < 6$, the system shows kinked-line configuration and behaves like a glass [24]. Starting with random initial configurations, we always end up with a metastable disordered structure as typified in Fig. 3(c), instead of the true ground state 3×3 . We expect a similar behavior in a realistic experiment with finite cooling rates: the system is trapped in one of the meta-stable states, showing a disordered configuration.

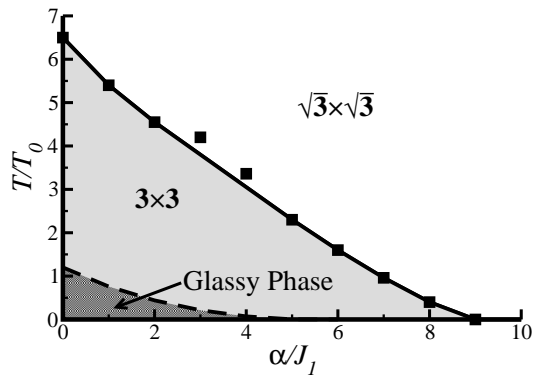


Figure 4: Phase diagram of the system. The boundary between the glassy phase and the 3×3 ground state is not well defined as indicated with the dashed line. $T_0 = J_1^2/\gamma$, $\delta = 0$.

Such behavior is directly related to the property of the single body potential of an adatom ,

$$\frac{1}{2}(\alpha - 6J_1)\tilde{z}_i^2 - \frac{\delta}{3}\tilde{z}_i^3 + \frac{\gamma}{4}\tilde{z}_i^4, \quad (7)$$

which develops a double-well shape when $\alpha/J_1 < 6$. As a result, the present model can be mapped onto an Ising antiferromagnet by considering the displacement \tilde{z}_i taking discrete values at the local minima of the double-well potential. Such an Ising antiferromagnet on a triangular lattice is known to have an exponentially large number of degenerate ground states [25]. Here, the vibrations of \tilde{z}_i around the local minima break the degeneracy, leading to the exponentially large number of meta-stable states in addition to its true ground state 3×3 .

The dependence of the stable configurations on α/J_1 qualitatively explains why the $\sqrt{3} \times \sqrt{3} \Leftrightarrow 3 \times 3$ transition is observed in the Sn/Ge and Pb/Ge systems, but not in Sn/Si: the stronger bond strength between a Sn adatom and a substrate Si atom places the system into the regime where $\alpha/J_1 > 9$. This is to be verified by future first-principles calculations.

The structural phase transition manifests itself by an accompanying charge density wave, as observed experimentally [1, 2]. Following the Hellmann-Feynman theorem, we obtain the total force acting on an adatom,

$$F_i = \alpha z_i - \beta \langle n_i \rangle + \mathcal{O}(z^3). \quad (8)$$

Setting $F_i = 0$ in equilibrium, we have $\langle n_i \rangle = \langle n \rangle + (\alpha/\beta)\tilde{z}_i + \mathcal{O}(\tilde{z}^3)$, showing that adatoms displaced upward gain electrons while those downward lose electrons.

We now study the finite temperature behavior of the system by applying the Monte-Carlo algorithm to the effective classical Hamiltonian shown in Eq. 4 along with Eq. 6. We find that the transition between the $\sqrt{3} \times \sqrt{3}$ phase and the 3×3 phase is of second-order with a sharply defined boundary, as shown in Fig. 4. There exists another boundary between the glassy phase and the 3×3 phase, which is the result of the glassy states at $T = 0$ when $\alpha/J_1 < 6$. As is typical in a

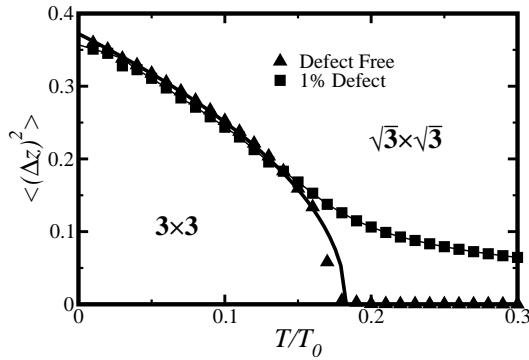


Figure 5: Temperature dependence of the order parameter for the defect-free system and the system with 1% defect. The thick solid line shows the function $A(1 - T/T_c)^{1/2}$ with $T_c/T_0 = 0.18$, $T_0 = J_1^2/\gamma$. The parameters are $\alpha/J_1 = 8.5$, $J_1 = 1$, $\gamma = 1.0$, and $\delta = 0.1$, with a simulation system size of 99×99 .

glassy system, the boundary of the glassy phase is not well defined. The detailed behavior of the $\sqrt{3} \times \sqrt{3} \Leftrightarrow 3 \times 3$ phase transition along the temperature axis is shown in Fig. 5. The order parameter is chosen as the mean square corrugation of the thermo-average positions of adatoms [21]. The defect-free system clearly shows a second-order transition from the 3×3 phase to the $\sqrt{3} \times \sqrt{3}$ phase as seen in Fig. 5, where the temperature dependence of the order parameter is well fitted by $A(1 - T/T_c)^{1/2}$. This behavior is different from the prediction of the Ginzburg-Landau type theories such as the CCM, which concludes that the critical behavior follows $|1 - T/T_c|$ [21].

Figure 5 also shows that the sharp phase transition in a pure system is blurred by the presence of a very low concentration of substitutional defects. In our calculations, the defect is simulated by introducing a constant displacement,

$$\Delta z = -\Delta\epsilon/\beta. \quad (9)$$

where $\Delta\epsilon$ is the site energy difference between a Ge substitutional defect and a Sn adatom [4]. As seen in Fig. 5, with only 1% defects, the sharp transition in the order parameter converts into a crossover behavior, explaining the experimental observation that the transition is gradual. Just like in the experiments [12, 21], our simulations show that each defect induces a local 3×3 patch above T_c , and the size of each individual 3×3 patch decreases gradually with the temperature.

In conclusion, we have presented a complete theory to understand the surface phase transitions observed in Sn/Ge (111) and Pb/Ge (111). Although we focus on these specific systems, the central ingredients of the theory, namely, the electron mediated indirect interaction and the resulting phonon instability, are conceptually much more general. These basic ideas, once properly applied, will enable us to gain better understanding of structural phase transitions in a wide class of

systems whose surfaces are metallic before the transition.

We gratefully acknowledge valuable discussions with A. Melechko, H. Weitering, Ismail, A. Chernyshev and Q. Niu. This work was supported in part by the LDRD of ORNL, managed by UT-Battelle, LLC for the USDOE (DE-AC05-00OR22725). It was also supported by the the NSF DMR-0105232 (EWP), DMR-0071893 (BW and ZZ) and the USDOE DE-FG03-01ER45687 (XCX).

-
- [1] J. M. Carpinelli, H. N. Weitering, E. W. Plummer, and R. Stumpf, *Nature* **381**, 398 (1996).
 - [2] J. M. Carpinelli, H. H. Weitering, M. Bartowiak, R. Stumpf, and E. W. Plummer, *Phys. Rev. Lett.* **79**, 2859 (1997).
 - [3] L. Petersen, Ismail, and E. W. Plummer (2002), to be published.
 - [4] T.-C. Chiang, M. Y. Chou, T. Kidd, and T. Miller, *J. Phy.: Cond. Matt.* **14**, R1 (2002).
 - [5] S. De Gironcoli, S. Scandolo, G. Ballabio, G. Santoro, and E. Tosatti, *Surf. Sci.* **454-456**, 172 (2000).
 - [6] O. Bunk, J. H. Zeysing, C. Falkenberg, R. L. Johnson, M. Nielsen, M. M. Nielsen, and R. Feidenhans, *Phys. Rev. Lett.* **83**, 2226 (1999).
 - [7] J. Zhang, Ismail, P. J. Rous, A. P. Baddorf, and E. W. Plummer, *Phys. Rev. B* **60**, 2860 (1999).
 - [8] G. Santoro, S. Scandolo, and E. Tosatti, *Phys. Rev. B* **59**, 1891 (1999).
 - [9] J. Avila, A. Mascaraque, E. G. Michel, M. C. Asensio, G. LeLay, J. Ortega, R. Perez, and F. Flores, *Phys. Rev. Lett.* **82**, 442 (1999).
 - [10] R. Peréz, J. Ortega, and F. Flores, *Phys. Rev. Lett.* **86**, 4891 (2001).
 - [11] G. Ballabio, G. Profeta, S. de Gironcoli, S. Scandolo, G. E. Santoro, and E. Tosatti, *Phys. Rev. Lett.* **89**, 126803 (2002).
 - [12] H. H. Weitering, J. M. Carpinelli, A. V. Melechko, J. Zhang, M. Bartkowiak, and E. W. Plummer, *Science* **285**, 2107 (1999).
 - [13] A. V. Melechko, J. Braun, H. H. Weitering, and E. W. Plummer, *Phys. Rev. B* **61**, 2235 (2000).
 - [14] M. A. Ruderman and C. Kittel, *Phys. Rev.* **96**, 99 (1954).
 - [15] T. L. Einstein and J. R. Schrieffer, *Phys. Rev. B* **7**, 3629 (1973).
 - [16] K. H. Lau and W. Kohn, *Surf. Sci.* **75**, 69 (1978).
 - [17] J. Repp, F. Moresco, G. Meyer, K.-H. Rieder, P. Hyldgaard, and M. Persson, *Phys. Rev. Lett.* **85**, 2981 (2000).
 - [18] W. A. Harrison, *Electronic structure and the properties of solids* (Dover, New York, 1989), p. 235.
 - [19] T. Holstein, *Ann. Phys. (N.Y.)* **8**, 325 (1959).
 - [20] B. Fischer and M. W. Klein, *Phys. Rev. B* **11**, 2025 (1975).
 - [21] A. V. Melechko, M. V. Simkin, N. F. Samatova, J. Braun, and E. W. Plummer, *Phys. Rev. B* **64**, 235424 (2001).
 - [22] G. Santoro, S. Scandolo, and E. Tosatti, *Comput. Mater. Sci.* **20**, 343 (2001).
 - [23] L. Petaccia, L. Floreano, M. Benes, D. Cvetko, A. Goldoni, L. Grill, A. Morgante, A. Verdini, and S. Modesti, *Phys. Rev. B* **63**, 115406 (2001).
 - [24] C. A. Angell, *Science* **267**, 1924 (1995).
 - [25] G. H. Wannier, *Phys. Rev.* **79**, 357 (1950).